IEEE Access
Multidisciplinary | Rapid Review | Open Access Journal

Received 6 February 2024, accepted 23 February 2024, date of publication 5 March 2024, date of current version 21 March 2024.

Digital Object Identifier 10.1109/ACCESS.2024.3374223

RESEARCH ARTICLE

Energy-Efficient FPGA Based Sleep Apnea Detection Using EEG Signals

MD. SHAMSHAD ALAM[1], YASRUB SIDDIQUI[1], MOHD HASAN[1], (Senior Member, IEEE), OMAR FAROOQ[1], (Senior Member, IEEE), AND YASSINE HIMEUR[2], (Senior Member, IEEE)

[1]Department of Electronics Engineering, Zakir Husain College of Engineering and Technology, Aligarh Muslim University, Aligarh 202002, India
[2]College of Engineering and Information Technology, University of Dubai, Dubai, United Arab Emirates

Corresponding author: Yassine Himeur (yhimeur@ud.ac.ae)

ABSTRACT Sleep apnea is a prevalent sleep disorder characterized by frequent interruptions in breathing during sleep, leading to decreased levels of blood oxygen. This research introduces an energy-efficient digital hardware system built on an Artix 7 FPGA, explicitly designed for real-time sleep apnea detection. Our approach involves the classification of subject-specific sleep apnea and non-apnea events. We utilize inter-band energy ratio features extracted from multi-band Electroencephalogram (EEG) signals and employ a Linear Support Vector Machine (LSVM) classifier for this task. The features extracted—namely energy, kurtosis, and mobility—from five sub-bands demonstrate improved accuracy, sensitivity, and specificity compared to existing studies. The proposed model is evaluated using EEG signals from the openly accessible St. Vincent's sleep apnea UCDDB database. Our system achieves remarkable performance metrics, attaining the highest accuracy of 94.81%, a sensitivity of 93.10%, and a specificity of 96.43%. It accomplishes all this while maintaining minimal dynamic power consumption (19mW) and using minimal FPGA resources. This hardware system can be integrated into a System-on-a-Chip (SoC) platform, serving as a crucial component of a smart, wearable, automated sleep apnea detection device for real-time critical health diagnosis and screening.

INDEX TERMS Wireless charging, wireless power transfer, dynamic wireless charging, vehicle-to-vehicle wireless charging, electric vehicles charging.

I. INTRODUCTION

Sleep apnea (SA) is a detrimental respiratory disorder characterized by recurrent breathing interruptions lasting around 10-20 seconds during sleep, accompanied by a marked decrease in blood oxygen saturation levels. It affects approximately 15% of men and 5% of women [1]. This disorder poses an elevated risk of numerous adverse health outcomes [2]. In its early stages, SA has immediate effects such as fatigue [3], intermittent hypoxia [4], irregular heart rates [5], and mood swings [6]. Prolonged exposure can escalate into severe complications, including cardiovascular issues [7], cognitive decline [6], strokes [8], and even mortality [9]. The American Association of Sleep Medicine (AASM) ranks sleep apnea among the top 10% of high-risk disorders leading to death [10]. A recent 18-year study at the University of Wisconsin-Madison revealed that individuals with SA are three times more likely to die from various diseases compared to those without SA symptoms.[1] Although treatments are available for Sleep apnea, still it remains undiagnosed and untreated in approximately 90% of affected individuals [11].

Sleep apnea, diagnosed and monitored through cardiorespiratory polysomnography (PSG), is classified into obstructive (OSA), central, and mixed types [12]. OSA occurs when muscle relaxation during sleep blocks the upper airway, leading to reduced or ceased airflow. Central sleep apnea is caused by neurological disorders affecting breathing signals [13], while Mixed Sleep Apnea (MSA) combines features of both. The severity of sleep apnea is measured

The associate editor coordinating the review of this manuscript and approving it for publication was Md. Kafiul Islam.

[1]https://aasm.org/

using the apnea-hypopnea index (AHI), which indicates the number of apnea and hypopnea episodes per hour of sleep [14]. Episodes typically last 30 to 60 seconds, causing blood oxygen desaturation and increasing health risks like heart issues, stroke, diabetes, depression, and headaches [15]. Therefore, developing reliable sleep apnea detection devices is vital for accurate diagnosis, ongoing monitoring, and effective management of these health risks [16].

The conventional method of polysomnography (PSG) for sleep apnea detection, despite being the gold standard, has significant drawbacks including patient discomfort, necessity for overnight lab stays, high costs, and time-consuming procedures. Addressing these challenges, this research proposes a cost-effective, energy-efficient, and portable biomedical system as an alternative, aiming to maintain PSG's diagnostic accuracy while enhancing monitoring convenience. Central to this approach is the use of Electroencephalogram (EEG) signals, which are crucial in detecting sleep apnea due to their ability to capture brain activity. EEG's effectiveness in reflecting brain electrical activity, vital for determining sleep stages and quality, makes it a focal point of research. Sleep apnea events, which severely impact sleep quality, highlight the need for precise EEG signal analysis for effective apnea detection [17], [18]. Recent research has advanced various methods for accurately identifying and classifying apnea using EEG signals. A notable study [19] introduced a subject-specific classification method using multi-band EEG signals and inter-band energy ratios. Employing the K-Nearest Neighbors (KNN) classifier, this method achieved a 92.2% accuracy rate and was evaluated using the St. Vincent's sleep apnea UCDDB database, underscoring the potential of EEG-based approaches in efficient and accurate sleep apnea detection.

The study by Lin et al. [20] utilized wavelet transform techniques to extract features from EEG signals for classifying apnea events, employing an Artificial Neural Network (ANN). By segmenting the EEG signal into five frequency bands and using the MIT-BIH polysomnographic database, they achieved a sensitivity of 69.64% and specificity of 44.44 In contrast, Gupta et al. [21] developed an automatic method to distinguish between apnea and non-apnea events, characterizing EEG signals with four parameters (energy, entropy, kurtosis, and mean absolute deviation) extracted from five frequency sub-bands. Utilizing an ensemble decision tree algorithm with bagging, they attained a peak accuracy of 95.10%, with a sensitivity rate of 93.20% and specificity rate of 96.80%, evaluated using the PhysioNET dataset. Another significant contribution by Hassan et al. [22] focused on single-channel EEG signals for automated sleep scoring. Their algorithm combined Ensemble Empirical Mode Decomposition (EEMD) with statistical moment-based feature extraction and implemented 'Random Under-Sampling Boosting' (RUSBoost) for classifying sleep stages. This method reached a notable accuracy of 98.15% for two-state sleep stages, using data from the Sleep-EDF database.

Vimala et al. [23] developed a system for detecting sleep apnea using single-lead EEG signals, focusing on three statistical parameters—energy, variance, and entropy—from decomposed EEG signals for classification. Utilizing machine learning (ML) classifiers like SVM, ANN, and KNN, they achieved the highest accuracy with SVM, at 95%, and excellent sensitivity and specificity rates. However, their study lacked a comparison with existing research. Ahmed et al. [24] introduced a technique to differentiate apnea from non-apnea episodes by analyzing fluctuations in the Beta band's temporal spectral energy. Employing a K-nearest neighbor classifier with these statistical features, they attained a peak accuracy of 82.28%, with high sensitivity and specificity. Bhattacharjee et al. [25] assessed the effectiveness of Rician model parameters and statistical measures in multi-band EEG signals, finding that entropy and log-variance were key feature parameters. The KNN classifier outperformed others in their study, achieving an accuracy rate of 91.02%, along with high sensitivity and specificity. Almuhammadi et al. [26] presented a hardware-based approach for diagnosing Obstructive Sleep Apnea (OSA) using EEG signal analysis. Their method, which involved filtering and decomposing EEG datasets into sub-bands, found the SVM algorithm to be the most accurate, with a classification accuracy of 97.14 These studies collectively demonstrate that various techniques and classifiers can effectively detect and classify sleep apnea events, offering diverse advantages and limitations.

Various ML models, including Convolutional Neural Networks (CNN) [27], Support Vector Machines (SVM) [28], K-Nearest Neighbors (KNN) [29], Artificial Neural Networks (ANN) [30], and Long Short-Term Memory (LSTM) [31], have been used for preprocessing medical data in sleep apnea detection. These methods typically integrate additional biomedical signals like ECG, SpO2, and EMG but rely on software models on server computers, leading to cost and performance limitations. This gap highlights the need for a real-time, hardware-based Computer-Aided Diagnosis (CAD) system for effective apnea detection. Field-Programmable Gate Arrays (FPGAs) are proposed for their processing speed, flexibility, power efficiency, parallel processing, and security [32], but their application in sleep apnea detection remains limited.

In another study, [33] utilized FPGA technology to create a sleep apnea detection hardware. This system employed a pre-trained Feedforward Neural Network (FNN) using SpO2 and ECG inputs for binary output but suffered from high power consumption of approximately 34W, limiting its portability. Moving forward, Paul et al. [34] developed real-time sleep apnea detection models using ECG and SpO2 signals. Their approach, using a simple feed-forward neural network, achieved a high cross-validation accuracy, especially with combined signals. Table 1 provides a comparative summary of these studies.

TABLE 1. Summary and comparison of existing related works to identify research gaps.

[20]	SAS detection	ANN	No	Sensitivity: 69.64%, Specificity: 44.44%	The effectiveness is heavily reliant on supervised learning methodologies, expert inputs for training, and a complex maintenance and retraining regime.
[21]	Apnea and non-apnea differentiation	Ensemble decision tree with bagging	No	Accuracy: 95.10%, Sensitivity: 93.20%, Specificity: 96.80%	The practical applicability may be limited by issues related to cross-validation, model complexity, signal dependency, and the need for broader comparisons and clinical validation.
[22]	Automated sleep scoring	RUSBoost	No	Accuracy: 98.15% (two-state sleep stages)	The class imbalance in sleep-EEG signal analysis could impact the classification performance, particularly for underrepresented sleep states. Additionally, generalization, reliance on single-channel data, and the need for technological implementation present further challenges.
[23]	Sleep apnea detection	SVM, ANN, KNN	No	SVM: Accuracy: 95%, Sensitivity: 100%, Specificity: 90%	The main limitations lie in the dataset's size and diversity, potential class imbalance issues, limited comparison with other classifiers, lack of external validation, specific focus on certain feature sets, and lack of detail on clinical applicability.
[24]	Apnea and non-apnea differentiation	KNN	No	Accuracy: 82.28%, Sensitivity: 90.58%, Specificity: 77.72%	The main drawback of this study lies in its limited scope of frequency bands, specific focus on sub-frame based analysis, small and potentially non-diverse sample size, lack of extensive validation across a broader population, and absence of discussion on clinical integration and real-world applicability.
[25]	Sleep apnea detection	KNN	No	Accuracy: 91.02%, Sensitivity: 98.28%, Specificity: 83.76%	The limitation sinclude the reliance on a limited dataset, potential overemphasis on a specific EEG frequency band, methodological complexity, questions about generalizability and applicability, and limited scope of comparison with other advanced methods.
[26]	Differentiating between patients with/without OSA	SVM	No	Accuracy: 97.14%	A small and potentially non-diverse sample size raises concerns about the generalizability, robustness, and clinical applicability of the findings.
[33]	Sleep apnea detection	FNN	Yes (Artix-7 FPGA)	Accuracy: 88%	Additionally, there is a high power consumption: 34W.
[34]	Real-time sleep apnea detection	FCNN	Yes (Artix-7 FPGA)	Cross-validation accuracy: 91.83 ± 1.51%	Lack extensive validation in real-world clinical settings, which is crucial to establish its efficacy and reliability for practical, non-invasive patient monitoring in neonatal intensive care units.

Despite recent advancements in the hardware implementation of sleep apnea detectors, the existing devices still have limitations in terms of accuracy and power consumption. Therefore, there is a need for a real-time, ML-based, energy-efficient device with high accuracy that can diagnose sleep apnea events at the point of care. This paper introduces an energy-efficient FPGA-based apnea detection system using EEG signals from the UCDDB PhysioNET database. The system, with low-complexity features extracted from specific EEG bands, achieves a 94% accuracy rate in detecting apnea through an LSVM classifier. This research aims to provide an intelligent, energy-efficient, fast automated sleep apnea detection system that reduces the workload and decision-making time for medical experts. The envisioned hardware system could function as an intelligent wearable device specialized in automated sleep apnea detection facilitating immediate and essential health assessments. To the best of our knowledge, this represents the first-ever FPGA implementation of a sleep apnea detector utilizing this specific database for evaluation and testing of sleep apnea using EEG signals. In this context, the proposed sleep apnea detector specifically targets Obstructive Sleep Apnea (OSA) due to its higher prevalence and greater recognition in comparison to central or mixed sleep apnea. Furthermore, a significant portion of both research and clinical efforts in the field, as documented in the literature [26], [27], [28], has been dedicated to devising effective treatments for OSA. Consequently, to ensure our findings are in harmony with the existing body of work, our research has prioritized the detection of OSA.

Typically, the primary goal of this project is to develop an energy-efficient, intelligent, and accurate sleep apnea detector. This device will be embedded in or integrated with an EEG headset band recorder for real-time operation. The initial phase of product development involves selecting suitable features and classifiers, along with their hardware implementation on an Artix-7 FPGA platform. This phase is crucial for enabling a fair comparison with existing architectures using a standard dataset. Subsequently, the project will progress to the integration of the FPGA with an

EEG headset to facilitate real-time testing of the prototype. Following comprehensive testing of the FPGA prototype, the design will be transitioned to an ASIC SoC to achieve higher energy efficiency and enhanced performance. This paper focuses on detailing the first stage of the project.

II. OVERVIEW OF THE PROPOSED WORK

The block diagram shown in Fig.1 illustrates the proposed methodology, demonstrating the hardware-software co-simulation process for efficient apnea detection hardware design. It emphasizes three critical steps: software simulation, hardware simulation, and performance analysis.

In the software simulation step, EEG data samples are collected and pre-processed. This processed data is subsequently divided into training, validation, and testing sets. The pre-processed data is then segmented into signals confined to specific frequency bands, from which distinct features are extracted. These features serve as input for the ML classifier model. After achieving optimal accuracy through various performance analyses, the learned parameters–namely weights and biases–are extracted from the trained model. These parameters are crucial in shaping the network architecture for the subsequent digital hardware implementation phase. In the hardware simulation stage, both the designed network architecture and the extracted parameters are implemented on a reconfigurable FPGA using the Xilinx Vivado design suite. This approach enables the translation of the proposed ML software model into an equivalent digital hardware system for apnea detection.

III. SOFTWARE SIMULATION

The software simulation process is illustrated through a flowchart depicted in Fig. 2. The initial step in creating an ML-based hardware system is to build and fine-tune the model in software to achieve optimal performance with real-time data. Prior to training the supervised ML model, essential steps like data collection, pre-processing, and labeling must be carried out.

The complete software simulation process consists of the following sequential steps: pre-processing, band decomposition, framing, feature extraction, and classification. All of these steps are first implemented using MATLAB, and then hardware implementation with the trained model parameters is carried out on FPGA. Complete description of all the steps involved in the software simulation process is given below:

A. PREPROCESSING

The preprocessing of EEG signals involves the removal of artefacts, which are unwanted signals or disturbances that can interfere with the accuracy of EEG data analysis. These artefacts commonly originate from eyeball movements, eye blinks, sweating, and body movements. During the preprocessing stage, a filtering technique is applied to the input EEG signal to eliminate these artefacts and facilitate feature extraction and classification. To preserve the EEG sub-band frequencies ranging from delta to beta bands, a fourth-order Infinite Impulse Response (IIR) Butterworth bandpass filter was created. This filter featured a passband spanning from 0.25 Hz to 40 Hz and operated at a sampling frequency of 128 Hz.

B. BAND-LIMITED SIGNAL EXTRACTION

During sleep, when a person experience pauses in breathing, there is a potential buildup of carbon dioxide in the blood. This accumulation reaches a critical level and is detected by specialized chemoreceptors. Upon detection, these receptors send signals to the brain, prompting the sleeping individual to awaken and inhale air. Consequently, this awakening trigger a transition in sleep stages, leading to variations in the activity levels across different frequency bands of the EEG signal. As a result, the utilization of frequency band-limited signals for apnea detection allows for preserving more distinctive features than analyzing the full-band EEG signal. Consequently, in the context of detecting apnea events, it is preferable to focus on the characteristics of band-limited signals rather than conducting analysis on the entire EEG signal. To facilitate this approach, the EEG signal is divided into five specific frequency bands, as shown in Fig. 2, namely delta (δ) (0.25-4 Hz), theta (θ) (4-8 Hz), alpha (α) (8-12 Hz), sigma (σ) (12-16 Hz), and beta (β) (16-40 Hz). The division of the EEG signal into these bands is achieved using the Butterworth band pass filter within the time domain, allowing for the interpretation of frequency components relevant to apnea detection. Fig. 3 portrays a plot of EEG signal in five Frequency Bands.

C. FEATURE EXTRACTION

Features play a crucial role in the classification of multiple classes by capturing fundamental characteristics essential for identification and differentiation among various classes. The processing of large volumes of EEG data poses a significant challenge in the field, necessitating the application of feature extraction techniques to reduce dimensionality and alleviate the computational load on the classifier. Frames of 10-second duration are considered to extract features from each sub-band. Specifically, for the classification of apnea and non-apnea events, the six simplest features are considered: energy, mobility, kurtosis, Skewness, interquartile range (IQR), and median absolute deviation (MAD), for each sub-band. These features are computed for a frame containing an EEG sample x_i with a length of 10 seconds as per the following equations:

$$Energy = \sum_{i=1}^{N} x_i^2 \tag{1}$$

$$Mobility = \sqrt{\frac{Var(x_i - x_{i-1})}{Var(x_i)}} \tag{2}$$

$$Kurtosis = \frac{\left(\frac{1}{N}\sum_{i=1}^{N}(x_i - x_{mean})^4\right)}{\left(\frac{1}{N}\sum_{i=1}^{N}(x_i - x_{mean})^2\right)^2} \tag{3}$$

$$IQR = Q_3 - Q_1 \tag{4}$$

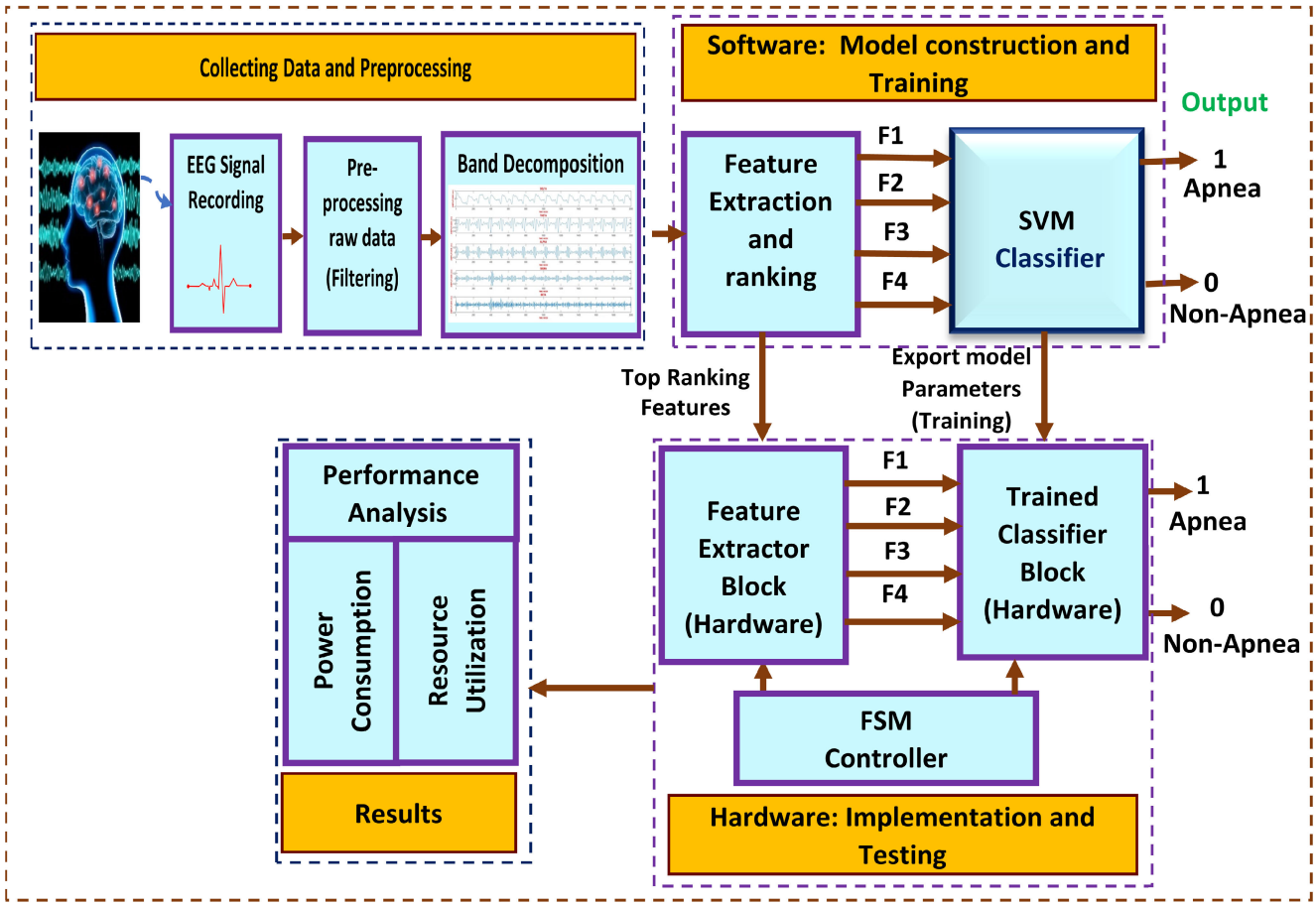

FIGURE 1. Block diagram of the proposed work.

$$MAD = median(|(x_i - m)|) \tag{5}$$

$$Skewness = \frac{\left(\frac{1}{N}\sum_{i=1}^{N}(x_i - x_{mean})^3\right)}{\left(\frac{1}{N}\sum_{i=1}^{N}(x_i - x_{mean})^2\right)^3} \tag{6}$$

where x_i represents a sample value obtained from the dataset. The variable m denotes the median of the dataset, while σ represents the standard deviation. Additionally, N signifies the total number of samples present in a frame. Moreover, Q_3 and Q_1 correspond to the upper quartile and lower quartile ranges, respectively.

Where x_i' represents a sample value obtained from the dataset. The variable m denotes the median of the dataset,, while σ represents the standard deviation. Additionally, N signifies the total number of samples present in a frame. Moreover, Q_3 and Q_1 correspond to the upper quartile and lower quartile ranges, respectively, while x_{mean} represents the average value (dc value) of the signals.

Since EEG signals represent the brain's electrical activity, so statistical features of these EEG signals offer valuable information about the brain's state. The computation of various statistical features yields significant information, enabling precise differences between apneic and normal conditions. The energy feature of EEG signals reflects the overall power or magnitude of the signal across different frequency bands. During an apnea, a bursting and quiescence in the overall energy or power of the EEG signal, particularly in higher frequency bands, is often observed. Mobility, another statistical feature, quantifies the amount of change or variation present in the EEG signal over time. In the context of EEG analysis, it signifies the movement or variability of the signal's frequency content. Apnea events tend to exhibit lower mobility compared to non-apnea events due to altered brain activity associated with breathing disturbances. Kurtosis, another important statistical measure, relates to the peak of the dataset and provides information about the presence of outliers or extreme values. In the case of EEG signals, kurtosis can indicate the presence of specific patterns or abnormalities associated with apnea events. The interquartile range (IQR) offers insights into the spread of values within the middle 50% of the dataset. In EEG signals, variations related to apnea may result in increased or decreased dispersion in certain frequency bands or signal segments. An increased IQR may indicate the presence of irregularities associated with apnea events. Additionally, the median absolute deviation (MAD) feature measures the

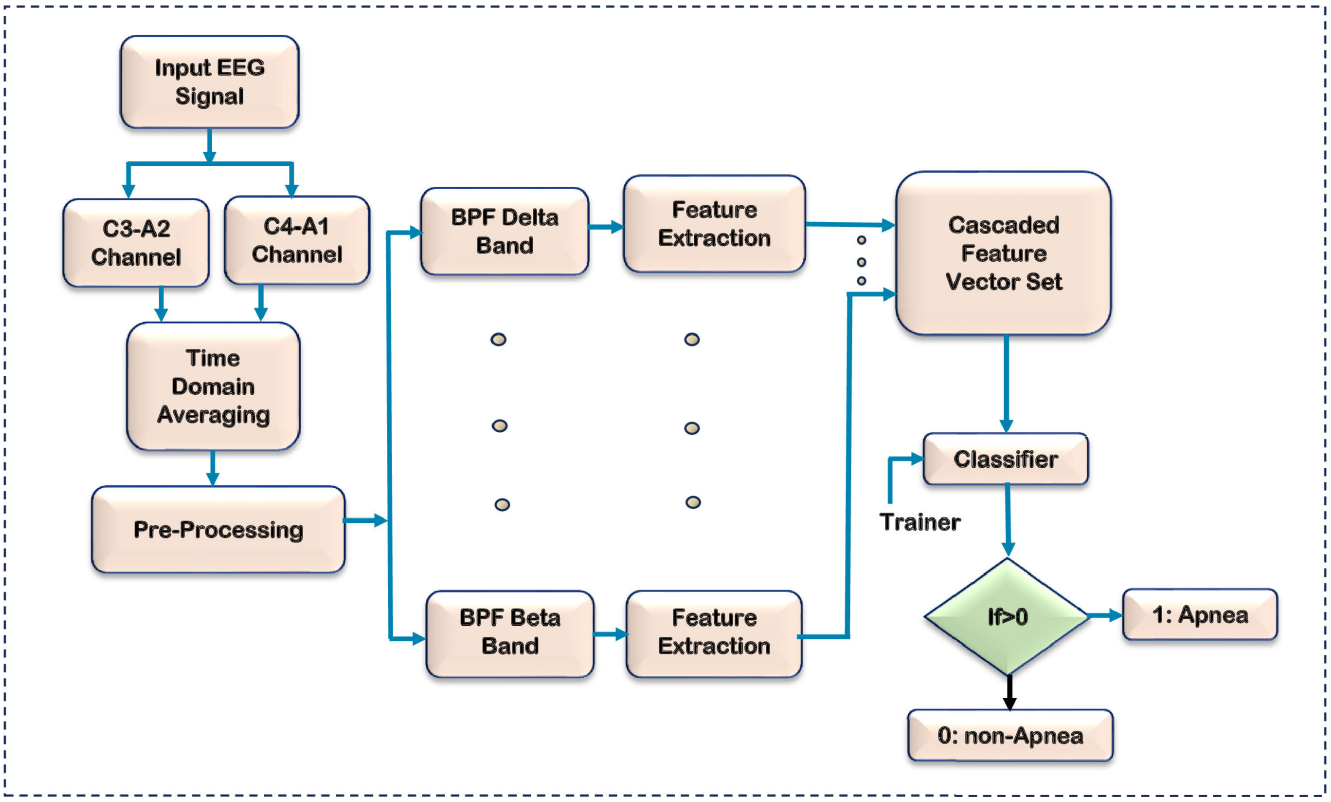

FIGURE 2. Flowchart illustrating the process of software simulation.

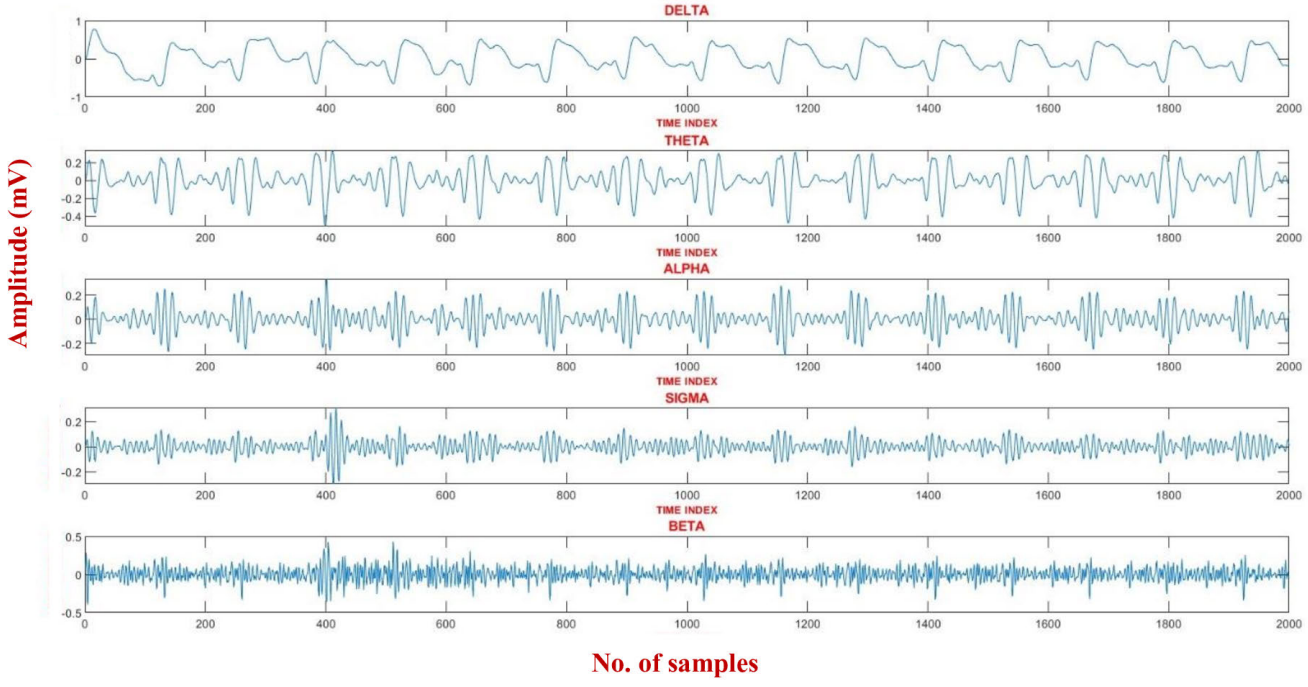

FIGURE 3. Plot of EEG signal in five frequency bands.

median absolute difference between each data point and the dataset's median. This robust measure of dispersion is less influenced by outliers compared to the standard deviation. In the context of EEG signals, MAD captures the signal's

variability or irregularity. Lastly, skewness is included in the feature vector set as a measure of the asymmetry of a probability distribution. Analyzing skewness values of EEG segments can aid in identifying abnormal patterns.

The resulting feature vector is formed by combining the six feature values extracted from each sub-band through concatenation. This comprehensive vector incorporates a total of 30 features originating from the examination of five sub-bands, with each sub-band contributing six distinct features. To assess their discriminative capacity and evaluate feature quality comprehensively, the set of 30 features is subjected to ranking. Ultimately, the top four ranked features–Energy beta, Kurtosis delta, Mobility delta, and Mobility beta–are selected as inputs to the subsequent classifier block.

IV. HARDWARE BLOCK FOR FEATURE EXTRACTION

The block diagram in Fig. 4 illustrates the complete hardware implementation of an apnea detector. The top four ranked features–Energy Beta, Kurtosis Delta, Mobility Delta, and Mobility Beta–are applied as inputs to the classifier block. The hardware implementation of the features extractor block is described as follows:

A. ENERGY

The block diagram in Fig. 5 illustrates the hardware implementation of the Energy feature. This implementation comprises an adder, a multiplier, and four registers. The sequential components within the feature extractor block are interconnected through reset and clock signals, which are controlled by a finite state machine (FSM) acting as a control unit. The process initiates with a high reset signal that resets all the resources within the block. When the reset signal transitions to low, the input data from the input buffer passes through the squarer block, producing an output that serves as one of the inputs for the adder circuit via Reg1. The second input of the adder circuit connects to the Reg2 block, which is initially set to zero. This configuration of the adder and Reg2 forms an accumulator. The sum of these two inputs is then stored back into Reg2, updating its value. This iterative process continues until the accumulator reaches the sum of all squared input values, resulting in the output known as energy. Finally, the energy output is stored in the output register (Out Reg1).

B. MOBILITY

The block diagram for the hardware implementation of the Mobility feature, displayed in Fig. 6, constitutes the lower half of the complete mobility block. The complete mobility block is divided into two halves. The upper half, shown in Fig. 5, represents the energy block responsible for generating energy, which serves as one of the inputs to the divider block used for computing mobility.

In the lower half of the Mobility block, as depicted in Fig. 6, the components are an adder, a subtractor, a multiplier, a divider, a square root block, six registers, and a control unit as the finite state machine (FSM). The subtractor calculates the difference between the present and delayed (past) input signals, and the result is saved as dx in Reg4. This dx output is then passed through the squarer block, resulting in the value of dx^2. The output of the squarer block serves as one of the inputs to the adder circuit, while the other input is connected to Reg6, which is initialized with a value of zero. The sum of these two inputs is stored back into Reg6, updating its value. This iterative process continues until the output register stores the sum of all its inputs. The finite state machine (FSM) activates a high-done signal, indicating that the final values of both register Out Reg 1 and Out Reg2 have been obtained at the input of the divider block. Subsequently, the output of the divider block becomes the input for the square root block, enabling the calculation of the Mobility feature.

The square root process in hardware involves the logic as follows: first, the radicand is divided into pairs of digits, starting from the least significant digit. Each pair consists of two bits. The first pair of digits is brought down. The pair is then subtracted from the previous result. If the subtraction result is not negative, the first answer digit is determined accordingly. Subsequently, the next pair of digits is brought down and appended to the previous result. The pair is subtracted from the extended result, and the result is analyzed. If it is negative, the corresponding answer digit is determined accordingly, and the result obtained in this step is discarded. This process continues until the last pair of digits, with each subsequent pair being brought down, appended to the previous result, and subtracted from the extended result. By using this logic, the square root of the number is determined.

C. KURTOSIS

The block diagram, shown in Fig. 7, shows the computation of the kurtosis feature. This block diagram consists of one adder, one divider, three multipliers, and five registers, along with the control unit known as the finite state machine (FSM). When the reset signal is low, the output of the energy block is directed to the squarer block, resulting in the output E^2, which is then stored in Reg12. This value serves as one of the inputs to the divider block. Simultaneously, the output of Reg1, as shown in Fig. 5, representing the squared value of the input signal (A), is connected to Reg8, which acts as the input to the squarer block, generating the output A^2. This output is then directed to the accumulator circuit through Reg10, serving as one of the inputs to the adder circuit, while the other input is connected to Reg9, initialized with a value of zero. The sum of these two inputs is stored back into Reg9, continuously updating its value through an iterative process. This iteration continues until the output register stores the sum of all its inputs. The final summation value is stored in Reg11, functioning as one of the inputs to the multiplier block, with the other input being a constant value N. The finite state machine (FSM) activates a high 'done' signal, indicating that the final values from the divider block are now

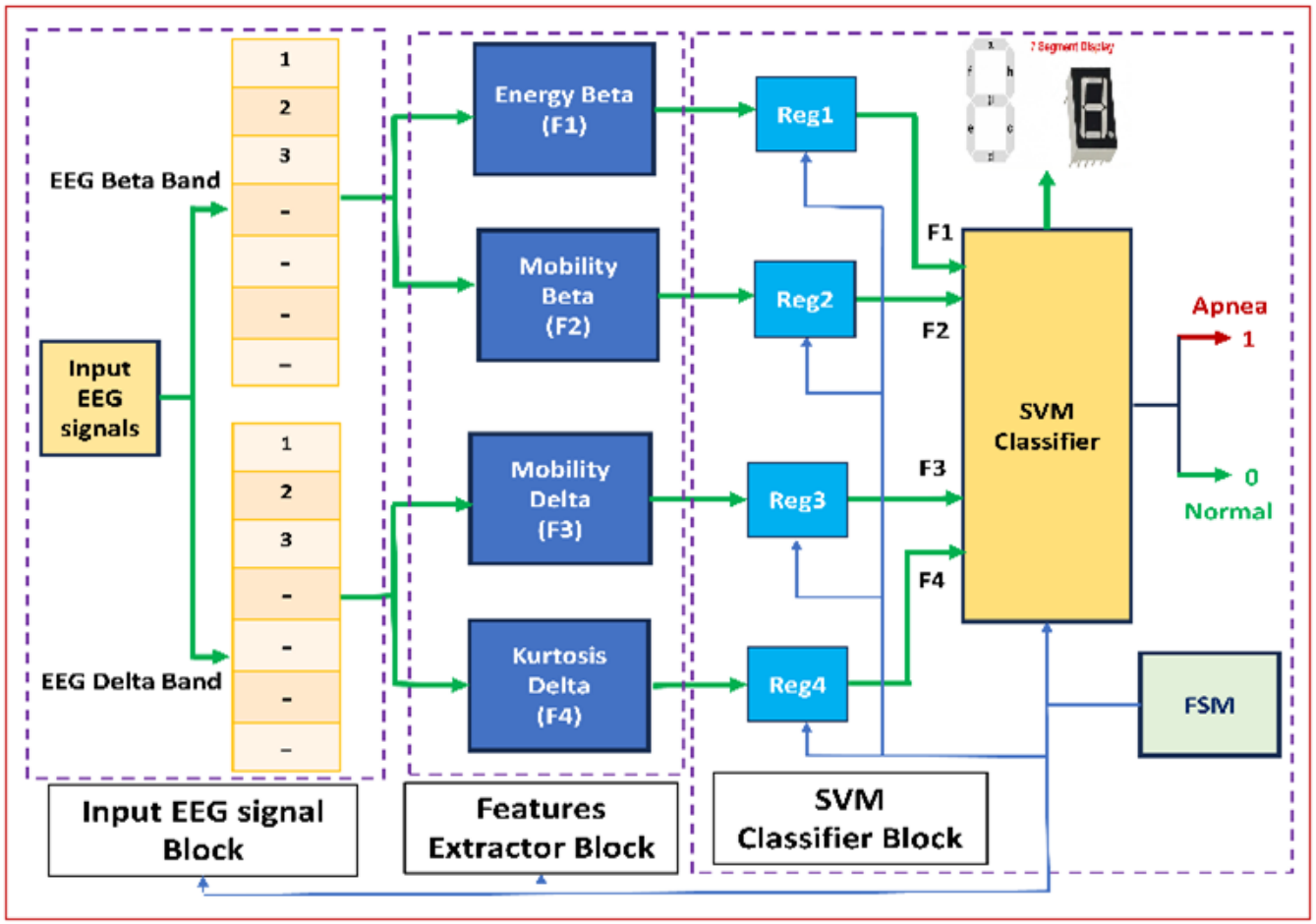

FIGURE 4. Block diagram depicting the hardware implementation of complete apnea detector.

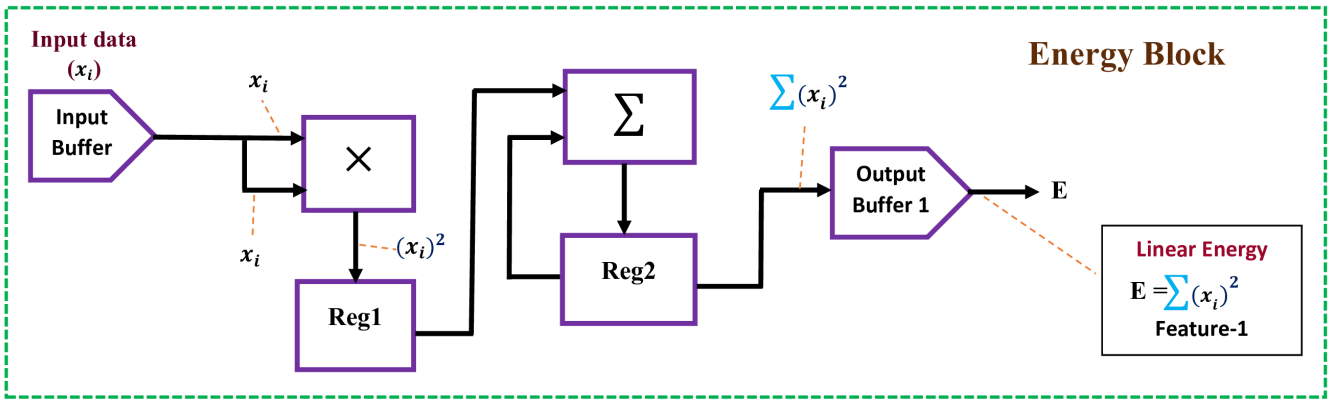

FIGURE 5. Block diagram depicting the hardware implementation of energy.

obtained at its input terminal. Finally, the divider block takes these two inputs and produces the output as kurtosis.

V. LINEAR SUPPORT VECTOR MACHINE CLASSIFIER

Support vector machines (SVMs) are powerful machine-learning algorithms for classification and regression analysis. Linear SVM is a subtype of SVM, designed for linearly separable datasets. The algorithm's importance lies in its ability to classify data by finding the optimal hyperplane to separate two classes of data points with the largest possible margin. This classifier's output is defined as follows in Equation 7.

$$z = wx + b \tag{7}$$

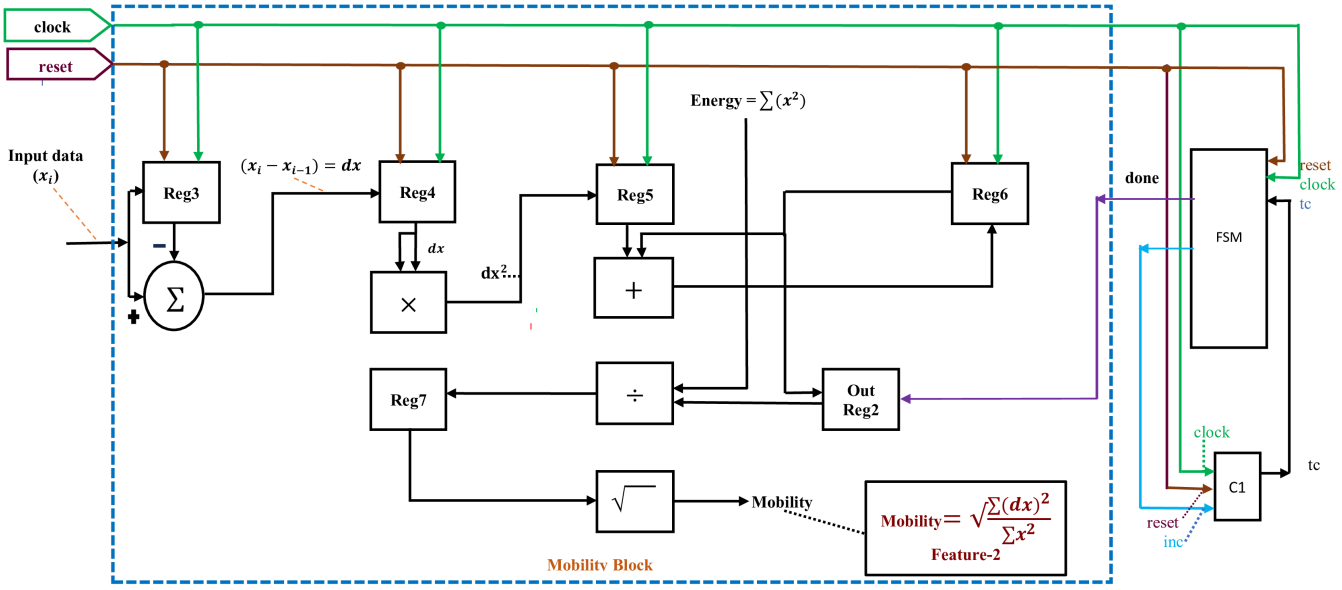

FIGURE 6. Block diagram depicting the hardware implementation of mobility.

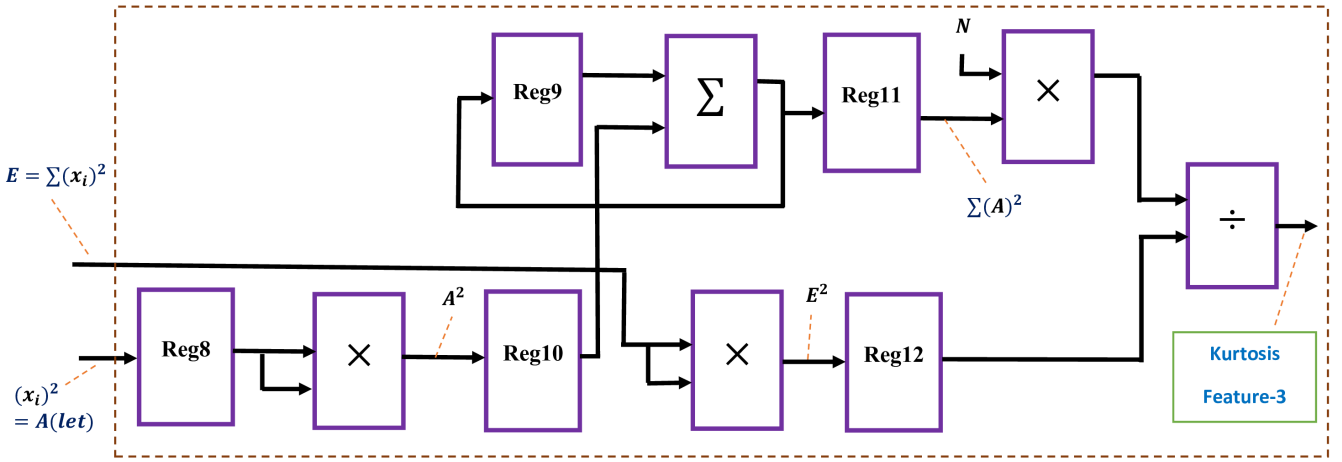

FIGURE 7. Block diagram for the hardware implementation of kurtosis.

where z is the predicted class, x is the input feature data, w is the weight vector that defines the hyperplane, and b is the bias term.

In the Linear SVM model, weight and bias are the two significant parameters that govern the position and orientation of the separating hyperplane. These values can be obtained by using Equations 8 and 9 respectively After extracting support vectors (x_i), Lagrange's approximation constant (α_i), and support vector labels (y_i), The weight is determined through the dot product of support vectors with their respective alpha values, followed by summation across all support vectors. The resulting weight value is then utilized to calculate the bias value.

$$w = \sum_{i=1}^{m} \alpha_i y_i x_i \tag{8}$$

$$b = -\frac{1}{2}\left(\min_{y_i=+1}(w \cdot x_i) + \max_{y_i=-1}(w \cdot x_i)\right) \tag{9}$$

Implementing linear SVM in hardware can offer advantages such as high-speed processing, low power consumption, and real-time decision-making capabilities. The implementation of Linear SVM in hardware involves a training process where the classifier is trained using the MATLAB tool. The training coefficients of the hyperplane are extracted and used for the hardware implementation of the model. Once the hardware model is trained with the training coefficients, it can be used for the classification of new data points based on the side of the hyperplane they fall on. A hardware model for the linear support vector machine classifier is obtained from Equation 7 as depicted in Fig. 8.

After training the classifier with the training data set, we get support vectors $\mathbf{x}_i$, Lagrange's approximation constant

TABLE 2. Subjects used for training.

S.No.	Subjects ID	AHI	No. of frames
1	UCDDB003	51	788
2	UCDDB011	8	88
3	UCDDB020	15	198
4	UCDDB024	24	390
5	UCDDB026	14	242

TABLE 3. Subjects used for test.

S.No.	Subjects ID	AHI	No. of frames
1	UCDDB007	12	214
2	UCDDB015	6	94
3	UCDDB018	2	28
4	UCDDB021	13	184
5	UCDDB022	7	58

α_i, and support vector labels $\mathbf{y}_i$. The weight is determined through the dot product of support vectors with their respective alpha values, followed by summation across all support vectors. The resulting weight value is then utilized to calculate the bias value. These weight and bias matrices are used in Equation 10 to implement the classifier on the hardware to find the predicted class.

$$z = (w_1 \cdot f_1 + w_2 \cdot f_2 + w_3 \cdot f_3 + w_4 \cdot f_4 + b) \tag{10}$$

VI. RESULT DISCUSSION

A. DATABASE DESCRIPTION

In this work, the FPGA implementation of the apnea detector utilizes a publicly available PhysioNET UCDDB database [34]. This database contains recordings for two EEG channels, C3-A2 and C4-A1, and their time-averaged values are taken into consideration. A sampling frequency of 128 Hz is utilized [34]. Irrespective of the type of apnea, the proposed method effectively distinguishes between apnea and non-apnea events. In this research, we have considered five commonly used subjects [21], [25], [35] exhibiting substantial differences in their Apnea-Hypopnea Index (AHI), and for each subject, a fixed number of apnea and non-apnea frames of duration 10 s are considered. In the software simulation, MATLAB R2021a is used to implement the proposed system. For the hardware implementation, the classifier model is trained using these five subjects, and a separate set of five new subjects is used to test the proposed hardware model. Detailed information about the subjects used for training and testing is shown in Table 2 and Table 3, respectively.

B. SIMULATION RESULTS

To evaluate the performance of the proposed model. the standard metrics such as accuracy, sensitivity, and specificity are calculated for each individual subject.

In order to evaluate the performance of the apnea classification system, a confusion matrix was generated, enabling the classification of data into true positives (TP), false positives (FP), true negatives (TN), and false negatives (FN).

The subject-specific results achieved through the implementation of the proposed features and SVM classifiers are meticulously compared with the results obtained from previous research works [21], [25], [35]. These comparisons are presented in Table 4. which presents the values of accuracy, sensitivity, and specificity for each subject, along with the averaged results across all five patients, employing the 5-fold cross-validation scheme. The presented table reveals that the proposed method exhibits significant improvements in sensitivity, specificity, and accuracy in comparison to the other published research work.

Table 5 presents a comprehensive comparison of mean classification results obtained using ten-fold, five-fold, and two-fold cross-validation methods. The objective is to evaluate the robustness of the classification outcomes in the presence of random variations in the training and test datasets. It is evident from the table that the proposed method consistently achieves better performance compared to the existing methods across all evaluation scenarios.

C. HARDWARE (FPGA) IMPLEMENTATION RESULTS

To evaluate the performance of the proposed hardware model, tests were conducted on five independent subjects to assess subject-specific accuracy, sensitivity, and specificity. We then calculated the average accuracy, sensitivity, and specificity across these subjects to gain a comprehensive understanding of the model's overall performance. For subject-independent accuracy, features from each subject, as listed in Table 2, were aggregated to form a training dataset for the classifier model. Testing was subsequently performed on five new independent subjects using their respective feature sets, as outlined in Table 3. Table 6 presents a comparative analysis of accuracy between the hardware model and software simulation model. The first three columns outline the independent testing accuracy, sensitivity, and specificity for each subject using the proposed hardware model. Meanwhile, the last column displays MATLAB simulation results for the same testing subjects. Surprisingly, the average accuracy of both hardware and software simulations is nearly identical, with only a minor difference observed. This subject-independent accuracy provides valuable insights into the performance of the proposed method, enhancing its reliability and applicability across different subjects.

The proposed model for apnea detection was implemented on a low-power consumption Artix-7 FPGA, identified by the part number xc7a15tcpg236-3. This specific board was chosen to facilitate a fair comparison with previous studies, as it is the same board used in most of the referenced works [33], [36] for their implementations. Detailed resource utilization summary is presented in Table 7. The report provides important information about the number of LUTs, slice registers, DSP blocks, block RAM, and I/O pins required for the proposed models' implementation. Additionally, the report highlights the percentage of resource utilization for each component.

The power requirements of the proposed models demonstrate a substantial reduction in power consumption, as indicated in Table 8. This power consumption report is generated

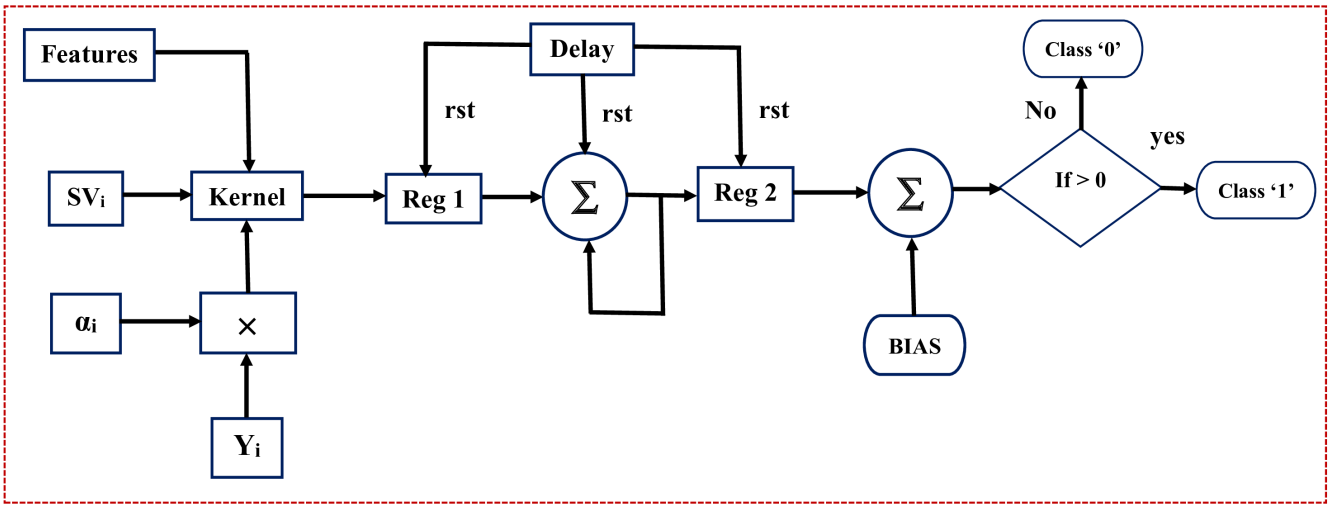

FIGURE 8. Block diagram of the linear support vector machine classifier.

TABLE 4. Comparision of the proposed work using LSVM classifier with energy ratio-based features (E [35]), rician model-based features (R [25]) and ensemble bagged trees classifier based-model (B [21]).

S.No.	Subject ID	Sensitivity (%)				Specificity (%)				Accuracy (%)			
		E [35]	R [25]	B [21]	Proposed	E [35]	R [25]	B [21]	Proposed	E [35]	R [25]	B [21]	Proposed
1.	UCDDB003	87.56	81.22	-	97.70	88.58	87.31	-	99.28	88.07	84.26	-	98.60
2.	UCDDB011	88.64	86.36	-	97.80	97.73	84.09	-	100.00	93.18	85.23	-	98.92
3.	UCDDB020	96.97	86.87	-	82.80	97.98	95.96	-	94.97	97.47	91.41	-	88.96
4.	UCDDB024	92.82	91.28	-	89.70	93.33	93.85	-	96.95	93.08	92.56	-	93.30
5.	UCDDB026	85.95	85.95	-	97.50	92.56	90.08	-	90.96	89.26	88.02	-	94.28
	Average	90.38	86.33	91.2	93.10	94.03	90.25	96.6	96.43	92.21	88.29	93.78	94.81

TABLE 5. Comparison on the basis of different cross-validation methods.

S.No.	Cross-Validation	Sensitivity (%)				Specificity (%)				Accuracy (%)			
		E [35]	R [25]	B [21]	Proposed	E [35]	R [25]	B [21]	Proposed	E [35]	R [25]	B [21]	Proposed
1.	2-fold	86.99	89.46	91.40	93.02	88.67	89.40	96.20	96.56	87.44	89.37	94.16	94.68
2.	5-fold	86.67	89.90	91.20	93.10	91.27	93.75	96.60	96.43	88.84	91.59	93.78	94.81
3.	10-fold	86.22	90.84	91.20	93.42	91.25	93.69	96.60	96.43	88.90	92.02	93.78	94.81

TABLE 6. Hardware and software testing results of 5-new subjects.

S.No.	Subject ID	FPGA Architecture Simulation			MATLAB Simulation Accuracy (%)
		Accuracy (%)	Sensitivity (%)	Specificity (%)	
1	UCDDB007	90.18	90.18	100	90.97
2	UCDDB015	89.47	78.72	100	90
3	UCDDB018	92.85	85.71	100	92.9
4	UCDDB021	93.47	86.95	100	96.7
5	UCDDB022	89.65	89.65	90	91.4
Average		**91.13**	**86.24**	**98**	**92.34**

at the post-implementation stage, incorporating the switching activity constraint file. The proposed apnea detection models exhibit the lowest level of dynamic power consumption, measuring 0.019 W at an operating frequency of 220MHz. A comparison has been made between the power consumption of our proposed seizure detector model and other seizure detector models referenced in the literature [34]. The presented outcomes reveal that our proposed model consumes less dynamic power, as well as less total on-chip power, compared to other architectures. To optimize power consumption and to achieve real-time applicability, our model implements a pipelined and low-switching activity architecture contrary to other mostly high-level Simulink-generated hardware architectures. As a result, our implemented model achieves

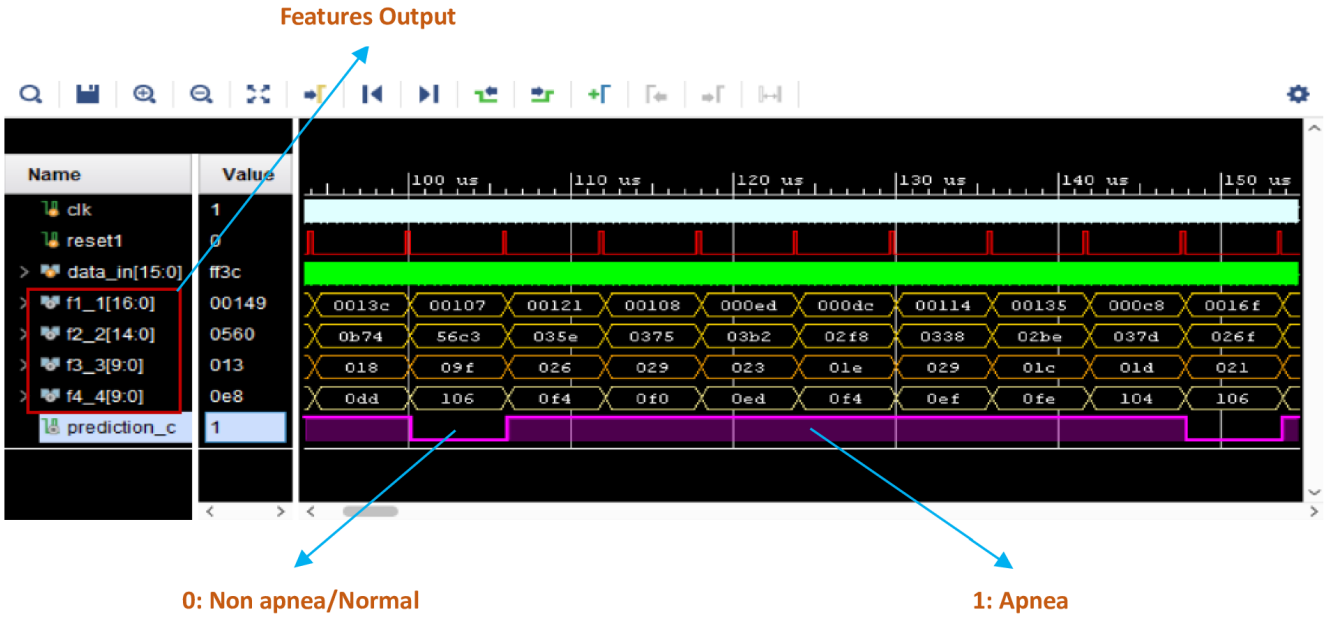

FIGURE 9. Simulation wave view of an apnea detector.

TABLE 7. Resource utilization.

Resource	Utilizing	Available	% Utilization
LUT	887	10400	8.53
FF	942	20800	4.53
DSP	9	45	20.00
IO	93	106	87.74

higher accuracy, sensitivity, and speed while consuming the least amount of power.

Fig. 9 visually illustrates the simulation window of the proposed architecture. It presents the wave-view of the LSVM-based seizure detection model. Inside this simulation window, the four features extracted from the feature extractor block, along with the apnea detection output labeled as ''prediction'' are displayed. The output is represented by low and high levels, where a high output signifies the presence of apnea, while a low output indicates a normal or non-apnea condition in the patients.

After conducting an extensive literature review, it appears that no prior research has focused on a hardware implementation of a sleep apnea detector utilizing the UCDDB PhysioNET database. Previous studies have solely reported software simulations using this database, presenting their results in terms of accuracy, sensitivity, and specificity, as shown in Tables 5 and 8.

D. ENERGY EFFICIENCY

The proposed architecture of the apnea detector is optimized at the RTL level by employing progressive bit sizing and pipelining techniques. Progressive bit sizing adjusts the bit size at each stage of the feature extraction process by truncating unused bits from both the integer and fractional parts, which significantly reduces power consumption during computation without compromising overall system accuracy. This technique is also incorporated within the classifier block, playing a pivotal role in hardware optimization. Pipelining segments tasks into multiple stages, enhancing throughput and reducing glitching power consumption. Through the combined application of these techniques, the proposed hardware architecture achieves outstanding accuracy while optimizing resource utilization and maintaining low dynamic power consumption. The power consumption of non-processor type FPGA architecture is mostly mentioned in terms of power consumed per clock cycle, along with latency, adopting the same performance criteria as existing FPGA architectures for fair comparison. TOPS/W and GOPS/W metrics are more commonly used with CPU/GPU-based accelerators in the ML domain.

VII. CONCLUSION

This paper introduces a highly energy-efficient and accurate FPGA-based apnea detection system, developed through a blend of software-hardware co-simulation techniques. The system employs EEG signals from the UCDDB PhysioNET database for analysis. We extract three low-complexity features—Energy, Mobility, and Kurtosis—from two specific EEG bands (beta and delta), chosen from the five available bands in the dataset. These features are subsequently fed into a Linear Support Vector Machine (LSVM) classifier, which adeptly identifies both apnea and non-apnea events. The entire design is implemented on the compact Artix-7 FPGA, with optimizations for low power consumption. Our proposed ML model achieves an average accuracy rate of approximately 94% in apnea detection. The system excels in multiple performance metrics, including speed, accuracy, sensitivity, and energy efficiency. Additionally, the

TABLE 8. Comparison based on different cross-validation methods.

ARTIX-7 FPGA Parameters	Power Consumption (W)			
	D.Pravin [37]	R.thaker [33]	O.Hasan [34]	Proposed work
Static Power	0.161	0.116	0.102	0.092
Dynamic Power	8.552	4.015	0.036	0.019
Total On-Chip Power	8.713	4.131	0.138	0.111
I/O Ports	4.283	0.77	0.016	0.001
Logic Gates	0.844	1.792	0.006	0.003
Signal/Registers	3.381	1.446	0.014	0.004
Thermal Margin	7.5	12.1	15.9	14.7

proposed architecture can be integrated into a System-on-a-Chip (SoC) platform, paving the way for the development of an intelligent, fast, and energy-efficient automated sleep apnea detection system. Implementing this high-accuracy on-chip predictive model also has the potential to alleviate the decision-making workload of medical professionals.

While the proposed method has shown significant achievements, Polysomnography (PSG) commonly induces discomfort in patients due to its wired connections and patch attachments. To address this issue, a wireless headset band designed for EEG recordings offers a practical solution. This state-of-the-art headset not only captures EEG signals with high effectiveness but also ensures smooth communication with the server, effectively eliminating the discomfort associated with conventional wired connections and patches. In our future work, we aim to integrate this headset band with an FPGA, facilitating real-time testing. This integration is expected to significantly enhance both the comfort and efficiency of the process.

REFERENCES

[1] P. E. Peppard, T. Young, J. H. Barnet, M. Palta, E. W. Hagen, and K. M. Hla, "Increased prevalence of sleep-disordered breathing in adults," *Amer. J. Epidemiol.*, vol. 177, no. 9, pp. 1006–1014, May 2013.

[2] V. K. Somers, D. P. White, R. Amin, W. T. Abraham, F. Costa, A. Culebras, S. Daniels, J. S. Floras, C. E. Hunt, L. J. Olson, T. G. Pickering, R. Russell, M. Woo, and T. Young, "Sleep apnea and cardiovascular disease: An American Heart Association/American College of Cardiology foundation scientific statement from the American Heart Association council for high blood pressure research professional education committee, council on clinical cardiology, stroke council, and council on cardiovascular NursingIn collaboration with the national heart, lung, and blood institute national center on sleep disorders research (National Institutes of Health)," *Circulation*, vol. 118, no. 10, pp. 1080–1111, Sep. 2008.

[3] V. K. Somers, D. P. White, R. Amin, W. T. Abraham, F. Costa, A. Culebras, S. Daniels, J. S. Floras, C. E. Hunt, L. J. Olson, and T. G. Pickering, "Pressure research professional education committee, council on clinical cardiology, stroke council, and council on cardiovascular nursing," *J. Amer. College Cardiol.*, vol. 52, no. 8, pp. 686–717, Aug. 2008.

[4] W. Chotinaiwattarakul, L. M. O'Brien, L. Fan, and R. D. Chervin, "Fatigue, tiredness, and lack of energy improve with treatment for OSA," *J. Clin. Sleep Med.*, vol. 5, no. 3, pp. 222–227, Jun. 2009.

[5] N. A. Dewan, F. J. Nieto, and V. K. Somers, "Intermittent hypoxemia and OSA: Implications for comorbidities," *Chest*, vol. 147, no. 1, pp. 266–274, Jan. 2015.

[6] P. K. Stein and Y. Pu, "Heart rate variability, sleep and sleep disorders," *Sleep Med. Rev.*, vol. 16, no. 1, pp. 47–66, Feb. 2012.

[7] M. Harris, N. Glozier, R. Ratnavadivel, and R. R. Grunstein, "Obstructive sleep apnea and depression," *Sleep Med. Rev.*, vol. 13, no. 6, pp. 437–444, Dec. 2009.

[8] J. Yeboah, S. Redline, C. Johnson, R. Tracy, P. Ouyang, R. S. Blumenthal, G. L. Burke, and D. M. Herrington, "Association between sleep apnea, snoring, incident cardiovascular events and all-cause mortality in an adult population: MESA," *Atherosclerosis*, vol. 219, no. 2, pp. 963–968, Dec. 2011.

[9] H. K. Yaggi, J. Concato, W. N. Kernan, J. H. Lichtman, L. M. Brass, and V. Mohsenin, "Obstructive sleep apnea as a risk factor for stroke and death," *Surv. Anesthesiolo.*, vol. 50, no. 2, pp. 102–103, Apr. 2006.

[10] T. Young, M. Palta, J. Dempsey, P. E. Peppard, F. J. Nieto, and K. M. Hla, "Burden of sleep apnea: Rationale, design, and major findings of the Wisconsin sleep cohort study," *Off. Publication State Med. Soc. Wisconsin*, vol. 108, no. 5, p. 246, 2009.

[11] T. Young, L. Finn, P. E. Peppard, M. Szklo-Coxe, D. Austin, F. J. Nieto, R. Stubbs, and K. M. Hla, "Sleep disordered breathing and mortality: Eighteen-year follow-up of the Wisconsin sleep cohort," *Sleep*, vol. 31, no. 8, pp. 1071–1078, 2008.

[12] Y. H. Khor, S.-W. Khung, W. R. Ruehland, Y. Jiao, J. Lew, M. Munsif, Y. Ng, A. Ridgers, M. Schulte, D. Seow, W. Soon, T. Churchward, and M. E. Howard, "Portable evaluation of obstructive sleep apnea in adults: A systematic review," *Sleep Med. Rev.*, vol. 68, Apr. 2023, Art. no. 101743.

[13] D. Parmenter and B. J. Millar, "How can general dental practitioners help in the management of sleep apnoea?" *Brit. Dental J.*, vol. 234, no. 7, pp. 505–509, Apr. 2023.

[14] H. Yu, D. Liu, J. Zhao, Z. Chen, C. Gou, X. Huang, J. Sun, and X. Zhao, "A sleep apnea-hypopnea syndrome automatic detection and subtype classification method based on LSTM-CNN," *Biomed. Signal Process. Control*, vol. 71, Jan. 2022, Art. no. 103240.

[15] A. Oksenberg and T. Leppänen, "Duration of respiratory events in obstructive sleep apnea: Factors influencing the duration of respiratory events," *Sleep Med. Rev.*, vol. 68, Apr. 2023, Art. no. 101729.

[16] Z. Zhuang, F. Wang, X. Yang, L. Zhang, C.-H. Fu, J. Xu, C. Li, and H. Hong, "Accurate contactless sleep apnea detection framework with signal processing and machine learning methods," *Methods*, vol. 205, pp. 167–178, Sep. 2022.

[17] Y. Elmir, Y. Himeur, and A. Amira, "ECG classification using deep CNN and gramian angular field," 2023, *arXiv:2308.02395*.

[18] T. Young, L. Evans, L. Finn, and M. Palta, "Estimation of the clinically diagnosed proportion of sleep apnea syndrome in middle-aged men and women," *Sleep*, vol. 20, no. 9, pp. 705–706, Sep. 1997.

[19] T. Schlüter and S. Conrad, "An approach for automatic sleep stage scoring and apnea-hypopnea detection," *Frontiers Comput. Sci.*, vol. 6, no. 2, pp. 230–241, Apr. 2012.

[20] R. Lin, R.-G. Lee, C.-L. Tseng, H.-K. Zhou, C.-F. Chao, and J.-A. Jiang, "A new approach for identifying sleep apnea syndrome using wavelet transform and neural networks," *Biomed. Eng., Appl., Basis Commun.*, vol. 18, no. 3, pp. 138–143, Jun. 2006.

[21] R. Gupta, T. F. Zaidi, and O. Farooq, "Automatic detection of sleep apnea using sub-band features from EEG signals," in *Proc. 3rd Int. Conf. Signal Process. Inf. Secur. (ICSPIS)*, Nov. 2020, pp. 1–4.

[22] A. R. Hassan and M. I. H. Bhuiyan, "Automated identification of sleep states from EEG signals by means of ensemble empirical mode decomposition and random under sampling boosting," *Comput. Methods Programs Biomed.*, vol. 140, pp. 201–210, Mar. 2017, doi: 10.1016/j.cmpb.2016.12.015.

[23] V. Vimala, K. Ramar, and M. Ettappan, "An intelligent sleep apnea classification system based on EEG signals," *J. Med. Syst.*, vol. 43, no. 2, p. 36, Jan. 2019.

[24] F. Ahmed, P. Paromita, A. Bhattacharjee, S. Saha, S. Azad, and S. A. Fattah, "Detection of sleep apnea using sub-frame based temporal variation of energy in beta band in EEG," in *Proc. IEEE Int. WIE Conf. Electr. Comput. Eng. (WIECON-ECE)*, Dec. 2016, pp. 258–261.

[25] A. Bhattacharjee, S. Saha, S. A. Fattah, W.-P. Zhu, and M. O. Ahmad, "Sleep apnea detection based on Rician modeling of feature variation in multiband EEG signal," *IEEE J. Biomed. Health Informat.*, vol. 23, no. 3, pp. 1066–1074, May 2019.

[26] W. S. Almuhammadi, K. A. I. Aboalayon, and M. Faezipour, "Efficient obstructive sleep apnea classification based on EEG signals," in *Proc. Long Island Syst., Appl. Technol.*, May 2015, pp. 1–6.
[27] J. V. Marcos, R. Hornero, D. Álvarez, F. del Campo, and C. Zamarrón, "Assessment of four statistical pattern recognition techniques to assist in obstructive sleep apnoea diagnosis from nocturnal oximetry," *Med. Eng. Phys.*, vol. 31, no. 8, pp. 971–978, Oct. 2009.
[28] B. Yılmaz, M. H. Asyalı, E. Arıkan, S. Yetkin, and F. Özgen, "Sleep stage and obstructive apneaic epoch classification using single-lead ECG," *Biomed. Eng. OnLine*, vol. 9, no. 1, p. 39, 2010.
[29] P. Varady, T. Micsik, S. Benedek, and Z. Benyo, "A novel method for the detection of apnea and hypopnea events in respiration signals," *IEEE Trans. Biomed. Eng.*, vol. 49, no. 9, pp. 936–942, Sep. 2002.
[30] D. Novak, K. Mucha, and T. Al-Ani, "Long short-term memory for apnea detection based on heart rate variability," in *Proc. 30th Annu. Int. Conf. IEEE Eng. Med. Biol. Soc.*, Aug. 2008, pp. 5234–5237.
[31] I. Mahbub, S. Islam, S. Shamsir, S. A. Pullano, A. S. Fiorillo, M. S. Gaylord, and V. Lorch, "A low power wearable respiration monitoring sensor using pyroelectric transducer," in *Proc. United States Nat. Committee URSI Nat. Radio Sci. Meeting (USNC-URSI NRSM)*, Jan. 2017, pp. 1–2.
[32] O. Azzouzi, M. Anane, M. Koudil, M. Issad, and Y. Himeur, "Novel area-efficient and flexible architectures for optimal ate pairing on FPGA," *J. Supercomput.*, vol. 80, no. 2, pp. 2633–2659, Jan. 2024.
[33] O. Hassan, R. Thakker, T. Paul, D. Parvin, A. S. M. Mosa, and S. K. Islam, "SABiNN: FPGA implementation of shift accumulate binary neural network model for real-time automatic detection of sleep apnea," in *Proc. IEEE Int. Instrum. Meas. Technol. Conf. (I2MTC)*, Ottawa, ON, Canada, May 2022, pp. 1–6.
[34] O. Hassan, S. Shamsir, and S. K. Islam, "Machine learning based hardware model for a biomedical system for prediction of respiratory failure," in *Proc. IEEE Int. Symp. Med. Meas. Appl. (MeMeA)*, Bari, Italy, Jun. 2020, pp. 1–5.
[35] S. Saha, A. Bhattacharjee, and S. A. Fattah, "Automatic detection of sleep apnea events based on inter-band energy ratio obtained from multi-band EEG signal," *Healthcare Technol. Lett.*, vol. 6, no. 3, pp. 82–86, Jun. 2019.
[36] M. S. Alam, M. Hasan, O. Farooq, and M. Hasan, "Field programmable gate array-based energy-efficient and fast epileptic seizure detection using support vector machine and quadratic discriminant analysis classifier," *Eng. Rep.*, Nov. 2023, Art. no. e12812.
[37] O. Hassan, D. Parvin, and S. Kamrul, "Machine learning model based digital hardware system design for detection of sleep apnea among neonatal infants," in *Proc. IEEE 63rd Int. Midwest Symp. Circuits Syst. (MWSCAS)*, Springfield, MA, USA, Aug. 2020, pp. 607–610.

MD. SHAMSHAD ALAM received the B.Tech. degree in electronics and communication engineering from the Maulana Azad College of Engineering and Technology, Patna, India, in 2012, and the M.Tech. degree in information technology from NIT Durgapur, Durgapur, India, in 2016. He is currently pursuing the Ph.D. degree with the Department of Electronics Engineering, Aligarh Muslim University, Aligarh, India. He received a Junior Research Fellowship from the University Grants Commission, New Delhi, India, in 2017.

YASRUB SIDDIQUI received the M.Sc. degree in electronics system and circuits design in India, in 2023. His research interests include low-power VLSI design, nanoelectronics, spintronics, and battery-less electron.

MOHD HASAN (Senior Member, IEEE) received the B.Tech. degree in electronics engineering from Aligarh Muslim University (AMU), Aligarh, India, in 1990, the M.Tech. degree in integrated electronics and circuits from Indian Institute of Technology Delhi (IIT Delhi), New Delhi, India, in 1992, and the Ph.D. degree in low-power architectures for multicarrier systems from The University of Edinburgh, Edinburgh, U.K., in 2004. He has been a full-time Professor with AMU, since 2005. He was a Visiting Postdoctoral Researcher on a project funded by the prestigious Royal Academy of Engineering, U.K., on low-power FPGA architecture with the School of Engineering, The University of Edinburgh. He has authored over 160 research papers in reputed journals and conference proceedings with an H-index of 26 and 2147 citations. His current research interests include low-power VLSI design, nanoelectronics, spintronics, and battery-less electron. He received the best international journal article and international conference paper awards.

OMAR FAROOQ (Senior Member, IEEE) received the Ph.D. degree from Loughborough University, Loughborough, U.K., in 2002. He is currently a Professor with the Department of Electronics Engineering, Aligarh Muslim University (AMU), Aligarh, India. He was an UKIERI Postdoctoral Fellow with Loughborough University, from 2007 to 2008. His research interest includes signal processing with focus on biomedical signal processing. He has authored/coauthored over 260 papers in journals and conferences. He is a fellow of the Acoustical Society of India (ASI) and the Institution of Electronics and Telecommunication Engineer (IETE), India.

YASSINE HIMEUR (Senior Member, IEEE) received the M.Sc. and Ph.D. degrees in electrical engineering, in 2011 and 2015, respectively. Following his doctoral studies, he obtained the Habilitation to Direct Research, which granted him the official authorization to supervise research, in July 2017. He is currently an Assistant Professor in engineering and information technology with the University of Dubai. His academic journey led him to join the faculty with the University of Dubai after serving as a Postdoctoral Research Fellow with Qatar University, from 2019 to 2022. Prior to that, he held the position of a Senior Researcher with the Algerian Center for Development of Advanced Technologies (CDTA), from 2013 to 2019, where he also served as the Head of the TELECOM Division, from 2018 to 2019. Throughout his career, he has been actively involved in conducting research and development projects and he has played a significant role in proposing and co-leading several research proposals under the NPRP Grant (QNRF, Qatar). With more than 90 research publications in high-impact venues, he has made valuable contributions to the field. He was honored to receive the Best Paper Award at the 11th IEEE SIGMAP in Austria, in 2014, and the Best Student Paper Award at IEEE GPECOM 2020, Turkey. His current research interests include big data and the IoT, AI/ML/DL, healthcare technologies, recommender systems, building energy management, and cybersecurity.